[Article] www.whxb.pku.edu.cn

N/F 掺杂和 N-F 双掺杂锐钛矿相 TiO_2(101)表面电子结构的第一性原理计算

陈琦丽 唐超群*
(华中科技大学物理系, 武汉 430074)

摘要: 采用密度泛函理论(DFT)平面波赝势方法计算了 N/F 掺杂和 N-F 双掺杂锐钛矿相 TiO_2(101)表面的电子结构. 由于 DFT 方法存在对过渡金属氧化物带隙能的计算结果总是与实际值严重偏离的缺陷, 本文也采用 DFT+*U*(Hubbard 系数)方法对模型的电子结构进行了计算. DFT 的计算结果表明 N 掺杂后, N 2*p* 轨道与 O 2*p* 和 Ti 3*d* 价带轨道的混合会导致 TiO_2 带隙能的降低, 而 F 掺杂以及氧空位的引入对材料的电子结构没有明显的影响. DFT+*U* 的计算却给出截然不同的结果, N 掺杂并没有导致带隙能的降低, 而只是在带隙中引入一个孤立的杂质能级, 反而 F 掺杂以及氧空位的引入带来明显的带隙能降低. DFT+*U* 的计算结果与一些实验测量结果能够较好地符合.

关键词: 锐钛矿相 TiO_2(101)表面; N/F 掺杂; 第一性原理计算; 电子结构
中图分类号: O649; O641; O472

First-Principles Calculations on Electronic Structures of N/F-Doped and N-F-Codoped TiO_2 Anatase (101) Surfaces

CHEN Qi-Li TANG Chao-Qun*
(*Department of Physics, Huazhong University of Science and Technology, Wuhan 430074, P. R. China*)

Abstract: Electronic structures of nitrogen (N)/fluorine (F)-doped and N-F-codoped TiO_2 anatase (101) surfaces were investigated by density functional theory (DFT) plane-wave pseudopotential method. Since DFT calculations performed on transition metal oxides always lead to a severe underestimation of the band gap, DFT+*U* (Hubbard coefficient) method was also adopted to calculate the electronic structures. DFT results demonstrated that mixing of N 2*p* states with O 2*p* and Ti 3*d* valence band (VB) states contributes to the band gap reduction of TiO_2 whereas F doping and the introduction of oxygen vacancies have no obvious effect on the electronic structure. However, from DFT+*U*, no obvious band gap narrowing was observed by N-doping except for the isolated N 2*p* states lying in the gap. In DFT+*U* calculation, F-doping as well as the introduction of oxygen vacancies leads to an obvious band gap narrowing. Results from DFT+*U* calculations accord well with some experimental results.

Key Words: TiO_2 anatase (101) surface; Nitrogen/fluorin-doped; First-principles calculation; Electronic structure

Titanium dioxide has received much attention as a promising photocatalytic semiconductor due to its excellent functionality, long-term stability, and nontoxicity[1]. However, as a wide band gap (3.2 eV[2]) semiconductor, it needs ultraviolet (UV) radiation to excite the electrons from valence band (VB) to conduction band (CB). Unfortunately, the energy of UV light is only about 8% of that of the sunlight. Then, how to enhance the visible light (Vis) sensitivity is critical to enable the utility of TiO_2 photocatalyst materials.

Many efforts have been made to achieve this purpose including introducing anionic species (C, N, F, P, and S) for doping. Some groups have reported that F-doped TiO_2 thin films showed

Received: December 3, 2008; Revised: February 7, 2009; Published on Web: March 18, 2009.
*Corresponding author. Email: cqtang@public.wh.hb.cn; Tel: +8627-87544351

a significant increase for the photodegradation activity under ir radiation of either UV or Vis[3–9]. Li *et al*.[8] have synthesized N-doped, F-doped, and N-F-codoped TiO_2 (NTO, FTO, and NFTO) powders by spray pyrolysis and they found that NFTO powder demonstrated an outstanding photocatalytic activity under both UV and Vis irradiation in the photocatalytic tests for degradation of acetaldehyde and trichloroethylene. The samples have been analyzed by UV-Vis absorption spectroscopy, photoluminescence (PL) spectra, and other experimental methods in order to elucidate the origin of their Vis-driven photocatalysis. The UV-Vis spectra indicated that the N-doping in NFTO did not cause the narrowing of the band gap of TiO_2, instead an isolated impurity energy state was formed near the VB. Whereas F-doping produced several beneficial effects including the creation of surface oxygen vacancies, the enhancement of surface acidity, and the increase of Ti^{3+} ions which contributed to the improvement of Vis sensitivity. The PL spectra provided confirmation that there were four electronic energy states existing between the VB and CB of NFTO which probably attributed to oxygen vacancies and doped N atoms. The experimental investigation on TiO_2 rutile (110) and anatase (101) single crystals performed by Batzill′s group[10] confirmed that N-doping introduced no band gap narrowing but localized N 2*p* states within the band gap just above the VB. Xu *et al*.[6] have prepared anatase FTO film by wet method which exhibited better photocatalytic activity in decomposing X-3B under artificial solar light. Their experimental tests showed that the high photocatalytic activity of FTO might due to extrinsic absorption through the creation of oxygen vacancies rather than the excitation of the intrinsic absorption of TiO_2. They also reported that F dopants incorporated into TiO_2 lattice might take a positive role in photocatalysis.

Additionally, Li *et al*.[3] have given theoretical calculation results for a $2\times2\times2$ TiO_2 anatase supercell which revealed that doped N atoms formed a localized energy state above the VB of TiO_2, whereas doped F atoms had no influence on the band structure. Wang *et al*.[11] and Lee *et al*.[12] have reported the calculations for N-doped TiO_2 anatase supercell with DFT method. Wang′s work[11] demonstrated that N doping introduced some states located at the maximum of VB, thus made band gap smaller. However, Lee *et al*.[12] thought the mixing of N(C) 2*p* states with O 2*p* VB states was too weak to produce a significant band gap narrowing. Unfortunately, we could not find more theoretical works on F doped and N-F-codoped TiO_2. Distinctly, these theoretical works performed in the case of TiO_2 bulk structure are not enough to explain the origin of high Vis activity of N/F doped or N-F-codoped TiO_2 essentially. Actually, the surface characteristics of a photocatalyst should be more closely related with its photocatalytic performances. It should be noted that there was few theoretical work on N/F doped or N-F-codoped TiO_2 surfaces. Therefore, in this present work, we focused on the electronic properties of N/F-doped and N-F-codoped TiO_2 anatase (101) surfaces in order to have a deep insight of the origin of their high Vis activity. The (101) surface is the predominant face of the anatase single-crystalline surfaces that is exposed on anatase minerals and polycrystalline powders, and theoretical calculation also showed that it was the thermodynamically low-energy surface[13,14].

1 Methods and models

1.1 Computational details

The computational calculations were performed within DFT plane-wave pseudopotential method[15] which has been used successfully on metal oxide surfaces in recent years[16−21]. The general gradient approximation (GGA) with PW91[22] functional and ultra-soft pseudo-potentials were used to describe the exchange-correlation effects and electron-ion interactions, respectively, with kinetic energy cutoff of 380.0 eV. The Brillouin zone sampling was restricted to the Γ point in surface geometry optimization and $7\times7\times3$ in bulk optimization calculations. In energy calculations, it was set to $1\times2\times4$. Structure optimization was performed by minimizing the total energy and the ionic force, until all the components of the residual forces were less than 0.1 eV·nm^{-1}. The energy and the displacement tolerance were set to 5.0×10^{-6} eV·atom^{-1} and 5.0×10^{-5} nm, respectively. All the calculations were performed in CASTEP codes[23].

However, DFT calculations performed in the case of transition metal oxide always lead to a severe underestimation of the band gap[24], even predict metallic behavior for systems that are known to be insulators or semiconductors[25,26]. An alternative methodology used to compensate for the limitation of DFT for those strongly correlated systems is DFT+*U* (Hubbard coefficient)[27], which introduces an additional term based on a simple Hubbard model for electron on-site repulsion. For energy calculation of TiO_2, the Coulomb correlation interaction of Ti 3*d* electrons should be taken account within DFT+*U*. The *U*=8.50 eV of Ti 3*d* electrons was used in Refs.[28,29], which has also been confirmed and used in the following calculations. Fig.1 demonstrated the density of states (DOSs) of bulk anatase with *U*=0.00 and 8.50 eV. We can see that the calculated band gap with *U*=0.00 eV is 2.12 eV. However, for the case of *U*=8.50 eV, it is 3.20 eV which is in agreement with the experimental value[2].

1.2 Models

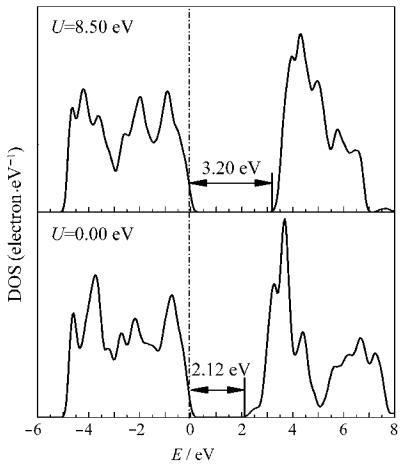

Fig.1 Density of states (DOSs) for bulk anatase TiO_2

The optimized TiO_2 (hereafter TiO_2 referring to the anatase structure exclusively) bulk lattice parameters are, a=0.3779 nm, c=0.9784 nm, and u=0.206, which agree well with the experimental values (a=0.3786 nm, c=0.9514 nm and u=0.208[30]). The calculated values have been used for the (101) surface calculations throughout the present work. The (101) surfaces were modeled by vacuum slabs. According to our previous computational results[31] and some references[32,33], we selected a slab of $Ti_{24}O_{48}$ (TO) with surface area of 1.115 nm×0.755 nm and slab thickness of 3 layers (Fig.2). The surface species, namely, the bridging two-fold coordinated oxygen atom (O_{2C}), three types of three fold coordinated oxygen atom (O^1_{3C}, O^2_{3C}, and O^3_{3C}) are denoted in Fig.2 as well.

Moreover, both experimental and theoretical studies demonstrated that N/F-doping into TiO_2 was likely to be accompanied by the oxygen vacancies[3,5–7,9,10,34] which were reported to play an important role in emerging visible light activity of the TiO_2 film[35,36]. So the cases of N/F-doped and N-F-codoped surfaces with an oxygen vacancy (VO) were also involved in the present work. There are three types of surface oxygen sites for the oxygen vacancy, doping N/F atoms to substitute. Thus, the vacancy formation energy (E_{vf}) and N/F substitutional energy (E_{sub}) for each site needed to be compared before the models were established.

E_{vf} is calculated as[37]:

$$E_{vf}=E_{\text{slab with an O vacancy}}+\frac{1}{2}E_{O_2}-E_{slab} \quad (1)$$

where E_{slab} and $E_{\text{slab with an O vacancy}}$ are the total energies of the surface and the surface having a VO, respectively, and E_{O_2} is the total energy of an isolated O_2 molecule which is calculated by putting an O_2 molecule in a 1 nm×1 nm×1 nm box.

E_{sub} is the cost of substitution of an oxygen atom with a nitrogen or fluorin atom which is calculated as:

$$E_{sub}=(E_{\text{A-doped slab}}+\frac{1}{2}E_{O_2})-(E_{slab}+\frac{1}{2}E_{A_2}) \quad (2)$$

where $E_{\text{A-doped slab}}$ is the total energy of the N/F-doped surface, E_{A_2} is the total energy of an isolated N_2/F_2 molecule calculated by putting a N_2/F_2 molecule in a 1 nm×1 nm×1 nm box. The values listed in Table 1 show that O_{2C} site is the most energetically favored for a fluorin atom or an oxygen vacancy to replace, whereas O^2_{3C} site is more active for a nitrogen atom to substitute. Thus the models for N/F-doped and N-F-codoped surfaces ($Ti_{24}O_{47}N$, $Ti_{24}O_{47}F$, and $Ti_{24}O_{46}NF$), which are denoted as NTO, FTO, and NFTO, respectively) were built by replacing an oxygen atom with a nitrogen atom at O^2_{3C} site and replacing an oxygen atom with a fluorin atom at O_{2C} site in the slab of TO. When discussing the surfaces having a VO, namely, $Ti_{24}O_{47}$, $Ti_{24}O_{46}N$, $Ti_{24}O_{46}F$, and $Ti_{24}O_{45}NF$, which are denoted as TO+VO, NTO+VO, FTO+VO, and NFTO+VO, respectively, and a bridging oxygen atom was removed to create a surface oxygen vacancy.

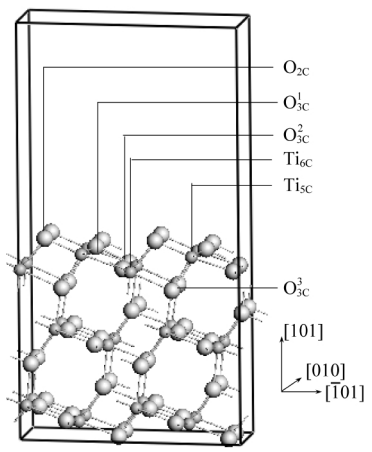

Fig.2 Structure of relaxed three-layer TiO_2(101) surface slab $Ti_{24}O_{48}$ (TO) with surface area of 1.115 nm×0.755 nm

Ti and O atoms are represented by small and big light grey spheres, respectively. Relevant surface species are indicated.

Table 1 Oxygen vacancy formation energies (E_{vf}) and N/F substitutional energies (E_{sub}) performed for different surface oxygen sites

Surface oxygen site	E_{vf}/eV	E_{sub}(N)/eV	E_{sub}(F)/eV
O_{2C}	4.93	3.20	−0.01
O^1_{3C}	6.00	3.07	0.36
O^2_{3C}	13.87	2.83	0.78

Positive (negative) value means an endothermal (exothermal) reaction.

Our calculation also confirmed the reduction of E_{vf} by introducing a nitrogen/fluorin dopant.

$$Ti_{24}O_{48}\rightarrow Ti_{24}O_{47}+\frac{1}{2}O_2,\ E_{vf}=4.93\ \text{eV} \quad (3)$$

$$Ti_{24}O_{47}N\rightarrow Ti_{24}O_{46}N+\frac{1}{2}O_2,\ E_{vf}=4.55\ \text{eV} \quad (4)$$

$$Ti_{24}O_{47}F\rightarrow Ti_{24}O_{46}F+\frac{1}{2}O_2,\ E_{vf}=3.88\ \text{eV} \quad (5)$$

2 Results and discussion

2.1 Electronic structures calculated with DFT

The density of states (DOSs) for TO, NTO, FTO, and NFTO, either for the surfaces having a VO, are shown in Fig.3, with the Fermi level being 0 eV on the energy axis. For the pure surface TO, the calculated band gap energy is about 2.6 eV (2.0 and 2.14 eV in Refs.[3] and [30]) which is much smaller than the experimental value (3.2 eV[2]) due to the well-known drawback of LDA and GGA[21]. The valence band consists of Ti 3*d* and O 2*p* orbitals with the width of 4.7 eV, and the conductive band consists of Ti 3*d* states mainly. For N-doped surfaces NTO and NFTO, N 2*p* states are found lying at the top of VB, which results in the width of VB expanding to about 5.2 eV and further leads a band gap narrowing from 2.6 eV to about 2.1 eV. However for FTO and NFTO, F 2*p* states are somewhat delocalized and involved in the bottom of VB, which takes no effect on the electronic structure. The results are similar to the theoretical results in Refs.[3,11,12].

It should be noted that both the introducing of VO and substitutional F-doping for a lattice O atom contribute excess electrons to the system, which converts the neighboring Ti^{4+} ions to Ti^{3+} ions. So, for the DOSs of FTO and the surfaces having a VO, the Fermi level moves to the bottom of CB and the systems exhibit *n*-type semiconducting behavior. From our previous work[31] and

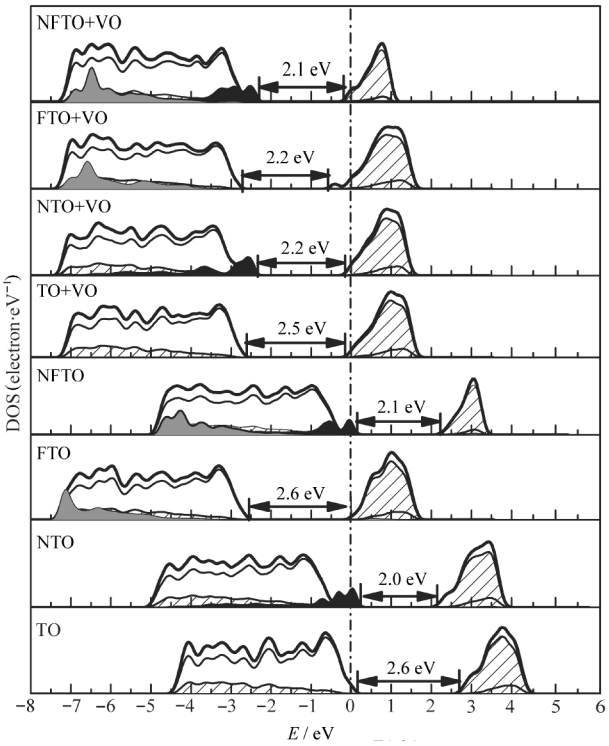

Fig.3 Density of the states (DOSs) calculated within DFT for the pure surface $Ti_{24}O_{48}$(TO), N-doped surface $Ti_{24}O_{47}N$(NTO), the F-doped surface $Ti_{24}O_{47}F$(FTO), N-F-codoped surface $Ti_{24}O_{46}NF$(NFTO), and surfaces having a bridging oxygen vacancy, namely, $Ti_{24}O_{47}$(TO+VO), $Ti_{24}O_{46}N$(NTO+VO), $Ti_{24}O_{46}F$ (FTO+VO) and $Ti_{24}O_{45}NF$(NFTO+VO)

some other reports[11,38], VO induced states were characterized by the presence of Ti^{3+} states which were found locating very close to the bottom of CB, about 0.2 −1.0 eV away. Although Ti^{3+} states can be easily observed lying close to the bottom of CB in the DOS of FTO+VO and result in a band gap narrowing from 2.6 to 2.2 eV which is likely because of the higher concentration of Ti^{3+} ions contributed by both VO and substitutional F-doping in the system. But Ti^{3+} states are not obvious in the DOSs of NTO+VO, NFTO+VO, and TO+VO. The comparison of the values of band gap of TO (2.6 eV) and TO+VO (2.5 eV), NTO (2.0 eV) and NTO+VO (2.2 eV), NFTO (2.1 eV) and NFTO+ VO (2.1 eV) indicate that the introducing of VO contributes little to band gap narrowing. Distinctly, the conclusion drawn from DFT calculation is that N-doping is responsible for the reduction of band gap of NTO, NTO+VO, NFTO and NFTO+VO, which does not accord with experimental observation[8,10] that N-doping can not introduce band gap narrowing of TiO_2.

2.2 Electronic structures calculated with DFT+*U*

The DOSs calculated within DFT+*U* are given in Fig.4. We can see that the band gap of the pure surface TO expands from 3.2 eV[2] to 3.5 eV. The width of VB is the same value of 4.7 eV as that obtained in DFT calculation. For NTO and NFTO, unlike that in DFT calculations, there is no obvious expansion of VB nor band gap narrowing observed. Some isolated N induced states are found lying in the gap and the peak is about 2.2 eV below the bottom of CB in NTO, 3.0 eV in NFTO. These results correspond to the experimental work reported by Nakano *et al*.[39], they found a new N-doping introduced state locating at 2.48 eV below the CB by deep-level optical spectroscopy measurement performed on N-doped TiO_2 films. Batzill[10] and Lee[12] *et al*. have also reported that the improvement of absorption of Vis of N-doped TiO_2 was due to isolated N 2*p* states above the maximum of VB of TiO_2 rather than due to a band gap narrowing experimentally and theoretically. For FTO, it is found that F 2*p* states are still delocalized and involved in the bottom of VB, but it is in contrast with the result obtained from DFT calculation that the mixing of F 2*p* states with O 2*p* and Ti 3*d* VB states leads to an obvious expansion of VB from 4.7 to 6.0 eV and a band gap narrowing from 3.5 to 2.5 eV, which indicates that F-doping takes a positive role in Vis response. Moreover, there are some isolated states lying in the middle of the gap and crossing the Fermi level. Such gap states are also observed from the DOSs of TO+VO, NTO+VO, FTO+VO, and NFTO+VO. Thus, one can conclude that these gap states crossing the Fermi level must be Ti^{3+} states introduced by VO and/or substitutional F-doping which used to locate at the bottom of CB in DFT calculations.

Besides the appearance of the gap states, an obvious band gap narrowing of 0.9 eV caused by the expansion of VB was also observed in TO+VO which indicates the introducing of VO may play an important role in band gap narrowing. It was proved by the DOSs of NTO+VO, FTO+VO and NFTO+VO. For NTO+VO, comparing with NTO, the width of VB expands from 4.7 to 5.5 eV and the band gap reduces from 3.5 to 2.5 eV. The majority of N 2*p* states keep lying in the gap whereas a small part of them are involved in the VB. In contrast with FTO, the band gap of FTO+VO drops from 2.5 to 2.3 eV. Interestingly, F 2*p* states have a shift to high energy and locate in the middle of VB. For NFTO+VO, F 2*p* states are observed showing the same distribution with that in FTO+VO, whereas most of N 2*p* states are involved in the top of VB, leading a slight expansion of VB of 0.3 eV by contrast with that in FTO+VO. Comparing with NFTO, the band gap of NFTO+VO drops from 3.5 to 2.0 eV which attributes to the introducing of VO mainly and the mixing of N 2*p* states with VB states also takes a positive effect. In conclusion, the introducing of VO either leads to a red shift of intrinsic absorption or produces extrinsic absorption and further enhances the Vis response. Moreover, NFTO+VO exhibits the largest red shift of intrinsic absorption which may give a proper explanation for the highest Vis activity of NFTO powder in photocatalytic test[8]. Although there is only one electronic energy state between VB and CB in the calculated DOS of NFTO, not as observed experimentally that there are four energy states in the gap[8], our theoretical results for NTO+VO, FTO+VO, and NFTO+VO confirm that the introducing of VO play an important role in the improved Vis activity of synthesized NTO, FTO, NFTO powders. Furthermore, we think the reason for the existence of VO resulting in a band gap narrowing is the excess electrons contributed

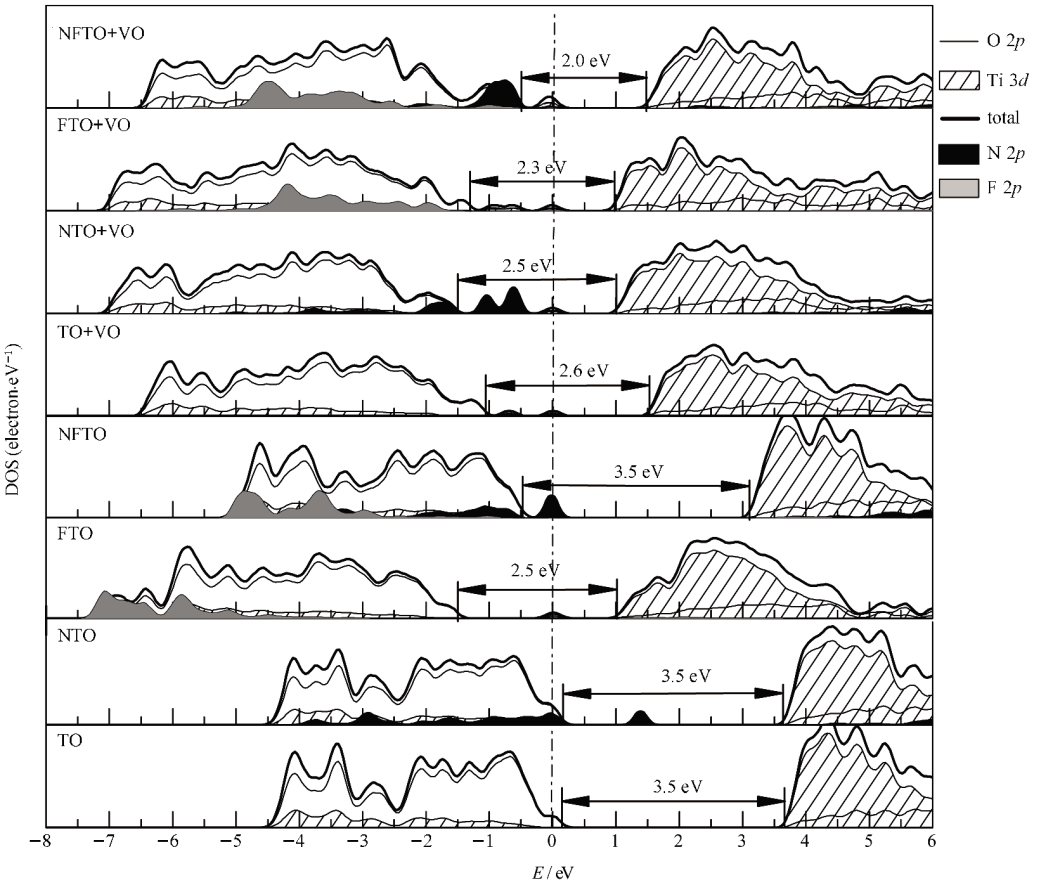

Fig.4 Density of states (DOSs) calculated with DFT+*U* for the pure surface $Ti_{24}O_{48}$(TO), N-doped surface $Ti_{24}O_{47}N$(NTO), F-doped surface $Ti_{24}O_{47}F$(FTO), N-F-codoped surface $Ti_{24}O_{46}NF$(NFTO), and surfaces having bridging oxygen vacancies, namely, $Ti_{24}O_{47}$ (TO+VO), $Ti_{24}O_{46}N$(NTO+VO), $Ti_{24}O_{46}F$(FTO+VO) and $Ti_{24}O_{45}NF$(NFTO+VO)

by VO to the system which increase repulsive interactions between VB electrons and then lead to an expansion of VB. That is why substitutional F-doping resulting in a band gap narrowing, too.

3 Conclusions

In this present work, density functional theory plane-wave pseudopotential method has been adopted to investigate the electronic properties of N/F-doped and N-F-codoped TiO_2 anatase (101) surfaces. The cases of the doped surfaces having an oxygen vacancy have been considered because of the reduction of oxygen vacancy formation energy by introducing N/F dopants. In order to overcome the limitation of DFT for transition metal oxides, DFT+*U* (Hubbard coefficient) method has also been used to get relative credible results.

The doping N induced states are found lying at the top of VB and the mixing of N 2*p* states with O 2*p* and Ti 3*d* VB states is confirmed to take a positive effect on band gap narrowing by leading to an expansion of VB with DFT method. DFT calculations also demonstrate that F 2*p* states take no effect on band gap narrowing, neither do the introducing of VO. Whereas DFT+*U* calculations gave different results. No obvious expansion of VB and band gap narrowing are observed by N-doping besides some isolated N 2*p* states lying in the gap. And the introducing of VO as well as F-doping was confirmed playing an important role in band gap narrowing. From the comparison of DFT and DFT+*U* calculations, we find that DFT+*U* calculations can give a better explanation for the reported experimental investigation that N-doping results in no band gap narrowing of TiO_2, whereas F-doping plays an important role in the improvement of Vis sensitivity of TiO_2. Although the results from DFT+*U* calculation do not correspond to the experimental observation completely, there is only one electronic energy state between VB and CB of NFTO predicted by DFT+*U* calculation, whereas experimental observation shows four energy states in the gap of NFTO, we think, besides substitutional anion-doping and surface vacancy considered in this work, there are more factors which may have effect on electronic properties of the synthesized photocatalyst, including interstitial anion-doping and surface anion/molecule adsorption. We will focus on this problem in our future research.

References

1 Diebold, U. *Surf. Sci. Rep.*, **2003, 48**: 53
2 Norton, D. P. *Mater. Sci. Eng. R-Rep.*, **2004, 43**: 139
3 Li, D.; Ohashi, N.; Hishita, S.; Kolodiazhnyi, T.; Haneda, H. *J. Solid State Chem.*, **2005, 178**: 3293

4 Todorova, N.; Giannakopoulou, T.; Romanos, G.; Vaimakis, T.; Yu, J. G.; Trapalis, C. *Int. J. Photoenergy*, **2008**: 534038

5 Wu, G. S.; Chen, A. C. *J. Photochem. Photobiol. A -Chem*., **2008, 195**: 47

6 Xu, J. J.; Ao, Y. H.; Fu, D. G.; Yuan, C. W. *Appl. Surf. Sci.*, **2008, 254**: 3033

7 Zhou, J. K.; Lv, L.; Yu, J. Q.; Li, H. L.; Guo, P. Z.; Sun, H.; Zhao, X. S. *J. Phys. Chem. C*, **2008, 112**: 5316

8 Li, D.; Haneda, H.; Hishita, S.; Ohashi, N. *Chem. Mater.*, **2005, 17**: 2596

9 Li, D.; Haneda, H.; Labhsetwar, N. K.; Hishita, S.; Ohashi, N. *Chem. Phys. Lett.*, **2005, 401**: 579

10 Batzill, M.; Morales, E. H.; Diebold, U. *Phys. Rev. Lett.*, **2006, 96**: 026103

11 Wang, Y.; Doren, D. J. *Solid State Commun.*, **2005, 136**: 186

12 Lee, J. Y.; Park, J.; Cho, J. H. *Appl. Phys. Lett.*, **2005, 87**: 011904

13 Vittadini, A.; Selloni, A.; Rotzinger, F. P.; Gratzel, M. *Phys. Rev. Lett.*, **1998, 81**: 2954

14 Lazzeri, M.; Vittadini, A.; Selloni, A. *Phys. Rev. B*, **2001, 63**: 155409

15 Payne, M. C.; Teter, M. P.; Ahan, D. C. *Rev. Mod. Phys.*, **1992, 64**: 1045

16 Franchini, C.; Bayer, V.; Podloucky, R. *Phys. Rev. B*, **2006, 73**: 155402

17 Fox, H.; Horsfield, A. P.; Gillan, M. J. *J. Chem. Phys.*, **2006, 124**: 134709

18 Li, Y. L.; Yao, K. L.; Liu, Z. L.; Gao, G. Y. *Phys. Rev. B*, **2005, 72**: 155446

19 Chatterjee, A.; Niwa, S.; Mizukami, F. *J. Mol. Graph.*, **2005, 23**: 447

20 Calatayud, M.; Minot, C. *J. Phys. Chem. B*, **2004, 108**: 15679

21 Muscat, J.; Harrison, N. M. *Phys. Rev. B*, **1999, 59**: 15457

22 Perdew, J.; Wang, Y. *Phys. Rev. B*, **1992, 45**: 13244

23 Segall, M. D.; Lindan, P. J. D.; Probert, M. J.; Pickard, C. J.; Hasnip, P. J.; Clark, S. J.; Payne, M. C. *J. Phys. -Condes. Matter*, **2002, 14**: 2717

24 Stampfl, C.; van de Wall, C. G. *Phys. Rev. B*, **1999, 59**: 5521

25 Anisimov, V. I.; Aryasetiawan, F.; Lichtenstein, A. I. *J. Phys.-Condens. Matter*, **1997, 9**: 767

26 Terakura, K.; Williams, A. R.; Oguchi, T.; Kubler, J. *Phys. Rev. B*, **1984, 30**: 4734

27 Dudarev, S. L.; Botton, G. A.; Savrasov, S. Y.; Humphreys, C. J.; Sutton, A. P. *Phys. Rev. B*, **1998, 57**: 1505

28 Gao, G. Y.; Yao, K. L.; Liu, Z. L. *Phys. Lett. A*, **2006, 359**: 523

29 Perebeinos, V.; Vogt, T. *Phys. Rev. B*, **2004, 69**: 115102

30 Howard, C. J.; Sabine, T. M.; Dickson, F. *Acta. Crystallogr. Sect. B-Struct. Sci*., **1991, 462**: 1347

31 Chen, Q. L.; Tang, C. Q.; Zheng, G. *Physica B*, **2009, 404**: 1074

32 Finazzi, E.; Di Valentin, C.; Selloni, A.; Pacchioni, G. *J. Phys. Chem. C*, **2007, 111**: 9275

33 Xu, Y. W.; Chen, K.; Liu, S. H.; Cao, M. J.; Li, J. Q. *Chem. Phys.*, **2007, 331**: 275

34 Di Valentin, C.; Pacchioni, G.; Selloni, A.; Livraghi, S.; Giamello, E. *J. Phys. Chem. B*, **2005, 109**: 11414

35 Ihara, T.; Miyoshi, M.; Iriyama, Y.; Matsumoto, O.; Sugihara, S. *Appl. Catal. B -Environmental*, **2003, 42**: 403

36 Justicia, I.; Garcia, G.; Vázquez, L.; Santiso, J.; Ordejón, P.; Battiston, G.; Gerbasi, R.; Figueras, A. *Sensors and Actuators B: Chemical*, **2005, 109**: 52

37 Oviedo, J.; San Miguel, M. A.; Sanz, J. F. *J. Chem. Phys.*, **2004, 121**: 7427

38 See, A. K.; Bartynsky, R. A. *J. Vac. Sci. Technol. A*, **1992, 10**: 2591

39 Nakano, Y.; Morikawa, T.; Ohwaki, T.; Taga, Y. *Appl. Phys. Lett.*, **2005, 86**: 132104